Sci Parasitol 23(1-2):29-43, April 2022
ISSN 1582-1366

New features complementing the descriptions of 7 species of acanthocephalans from South America, Vietnam, Iran, and Europe

Omar M. Amin[1]✉, Richard A. Heckmann[2]

1 – Institute of Parasitic Diseases, 11445 E. Via Linda 2-419, Scottsdale, Arizona 85259, USA.
2 – Department of Biology, Brigham Young University, 1114 MLBM, Provo, Utah 84602, USA (deceased).
Correspondence: omaramin@aol.com; +480-767-2522; +480 767-5855 (fax)

Abstract. Our examination of recent submissions revealed that new features and records were not included in our descriptions of 7 species of acanthocephalans collected from Europe, South America, Vietnam, and Iran. These features are herein presented to supplement already published descriptions thus rendering the accounting of each of the species complete. SEM and some microscope images that were never before published are provided for *Acanthocephalus rhinensis* Amin, Thielen, Munderle, Taraschewski, Sures, 2008 (Echinorhynchidae), *Centrorhynchus globocaudatus* (Zeder, 1800) Lühe, 1911 (Centrorhynchidae), *Corynosoma strumosum* (Rudolphi, 1802) Lühe, 1904 (Polymorphidae), *Sphaerorostris picae* (Rudolphi, 1819) Golvan, 1956 (Centrorhynchidae), *Rhadinorhynchus oligospinosus* Amin, Heckmann, 2017 (Rhadinorhynchidae), *Australorhynchus multispinosus* Amin, Heckmann, Ha, 2019 (Gorgorhynchinae), and *Tenuisentis niloticus* (Meyer, 1932) Van Cleave, 1936 (Tenuisentidae). Images of hyperparasite microsporidians in *C. globocaudatus*, among other newly described features are also included.

Keywords: Acanthocephala; Supplementing descriptions; SEM; New features.

Caracteristici noi care completează descrierile a 7 specii de acantocefali din America de Sud, Vietnam, Iran şi Europa

Rezumat. Examinarea publicaţiilor recente a arătat că noi caracteristici şi înregistrări nu au fost incluse în descrierile noastre privind 7 specii de acantocefali colectate din Europa, America de Sud, Vietnam şi Iran. Aceste caracteristici sunt prezentate aici pentru a completa descrierile deja publicate, făcând astfel descrierea fiecărei specii completă. SEM şi unele imagini la microscop, care nu au fost niciodată publicate până acum, sunt furnizate pentru *Acanthocephalus rhinensis* Amin, Thielen, Munderle, Taraschewski, Sures, 2008 (Echinorhynchidae), *Centrorhynchus globocaudatus* (Zeder, 1800) Lühe, 1911 (Centrorhynchidae), *Corynosoma strumosum* (Rudolphi, 1802) Lühe, 1904 (Polymorphidae), *Sphaerorostris picae* (Rudolphi, 1819) Golvan, 1956 (Centrorhynchidae), *Rhadinorhynchus oligospinosus* Amin, Heckmann, 2017 (Rhadinorhynchidae), *Australorhynchus multispinosus*

Amin, Heckmann, Ha, 2019 (Gorgorhynchinae) şi *Tenuisentis niloticus* (Meyer, 1932) Van Cleave, 1936 (Tenuisentidae). Sunt incluse şi imagini ale microsporidienilor hiperparaziţi ale *C. globocaudatus,* printre alte caracteristici nou descrise.

Cuvinte cheie: Acanthocephala; Descrieri suplimentare; SEM; Noi trăsături.

Received 03.03.2022. Accepted 28.04.2022.

Introduction

A review of recent submissions of published accounts revealed that some significant taxonomic aspects represented by SEM images were not included in the description of a good number of acanthocephalan species. Much of the purported rational had to do with keeping the number of pages down ("boil it down" as editors often say) as our publications tend to be large with numerous pages and figures. The final published products often missed features that we now feel need to be added to complement the original descriptions. Table 1 includes 7 such accounts from Europe, Iran, Vietnam, and Peru; see text for references. Now, we feel that our presented descriptions are finally complete. Our review will include additional features in other species of acanthocephalans that will be addressed in due time.

Materials and methods

Microscopical methods

Freshly collected acanthocephalans were extended in water until proboscides were everted then fixed in 70% ethanol for transport to our Institute of Parasitic Diseases (IPD) in Arizona, USA for processing and further studies. Worms were punctured with a fine needle and subsequently stained in Mayer's acid carmine, de-stained in 4% hydrochloric acid in 70% ethanol, dehydrated in ascending concentrations of ethanol reaching 100% (24 hr each), and cleared in 100% xylene then in 50% Canada balsam and 50% xylene (24 hr each). Whole worms were then mounted in Canada balsam.

Microscope images

Microscope images were created using 10X and 40X objective lenses of a BH2 light Olympus microscope (Olympus Optical Co., Osachi-shibamiya, Okaya, Nagano, Japan) attached to an AmScope 1000 video camera (United Scope LLC, dba AmScope, Irvine, California), linked to an ASUS lab top equipped with HDMI high-definition multimedia interface system (Taiwan-USA, Fremont, California).

Images from the microscope are transferred from the lab top to a USB and stored for subsequent processing on a computer.

Scanning electron microscopy (*SEM*)

Specimens that had been fixed and stored in 70% ethanol were processed for SEM following standard methods (Lee, 1992). These included critical point drying (CPD) in sample baskets and mounting on SEM sample mounts (stubs) using conductive double-sided carbon tape. Samples were coated with gold and palladium for 3 minutes using a Polaron #3500 sputter coater (Quorum (Q150 TES) www.quorumtech.com) establishing an approximate thickness of 20 nm.

Samples were placed and observed in an FEI Helios Dual Beam Nanolab 600 (FEI, Hillsboro, Oregon) Scanning Electron Microscope with digital images obtained in the Nanolab software system (FEI, Hillsboro, Oregon) and then stored on a USB for future reference. Samples were received under low vacuum conditions using 10 KV, spot size 2, 0.7 Torr using a GSE detector.

Results and discussion

Acanthocephalus rhinensis Amin, Thielen, Munderle, Taraschewski, Sures, 2008 (figures 1-6)

Amin et al. (2008) described *A. rhinensis* from the European eel *A. Anguilla* in the Rhine River near the City of Karlsruhe, Germany (table 1) and provided a key to the identification of species of the genus *Acanthocephalus* Koelreuther, 1771 in Europe. Amin et al. (2008) also provided 6-line drawings of an adult male, adult female, proboscis, 3 proboscis hooks and roots nos. 1, 7, 13 of 1 row, female reproductive system, and an egg. In addition to its distinguishing characteristics of hook formula and size and shape of testes, lemnisci, and eggs, freshly collected specimens of *A. rhinensis* exhibited a characteristic orange-brown band encircling the anterior end of the trunk (figure 8 of Amin et al., 2008, p. 1302). We now provide the first set of SEM images of *A. rhinensis* from the same collection showing the proboscis (figure 1), terminal female gonopore (figures 2, 4), and egg (figure 3), and 2 images of micropores from anterior trunk (figure 5) and from posterior trunk (figure 6). Note the difference in micropore diameter and distribution in the 2 trunk regions. The only other SEM images of *A. rhinensis* are those of the proboscis and hooks of adults and cystacanths from *A. anguilla* and from the amphipod *Echinogammarus tibaldii* Pinkster and Stock, respectively, collected from Lake Piediluco, Central Italy (Dezfuli et al., 2012). The characteristic orange-brown pigmentation encircling the anterior end of the trunk observed in our German specimen was absent in the Italian material.

Centrorhynchus globocaudatus (Zeder, 1800) Lühe, 1911 (Centrorhynchidae) (figures 7-18)

Amin et al. (2020) presented the most comprehensive treatment of the morphology, molecular biology, and Energy Dispersive x-ray analysis of *C. globocaudatus* utilizing specimens collected from *Falco tinnunculus* Linn. and *Buteo buteo* Linn. in northern Italy. In another collection, we report here, for the first time, 3 specimens of *C. globocaudatus* from 1 long-legged buzzard *Buteo rufinus* Cretzschmar in Sabzevar Razavi Khorasan Province, Iran. These specimens provided SEM images (figures 7-12) and images of a microsporidian hyperparasite (figures 13-18); all are new geographical and host records in Iran. A proboscis broader posteriorly and partially retracted anteriorly, and typical proboscis hooks from another specimen are shown in figures 7 and 8, respectively. An egg revealing subsurface filaments is shown in figure 9. The variability in micropore diameter and distribution is well represented in figures 10-12 magnified to the same scale from different trunk regions demonstrate differences in nutrient absorption rates. Heckmann et al. (2013) analyzed these relationships very well in 16 species of acanthocephalans including *C. globocaudatus*. In most cases, "the highest number and largest pore size occurred in the midbody of the acanthocephalans" (Heckmann et al., 2013, p. 105).

Hyperprasitism has been demonstrated in a number of parasites infected with hyperparasites including the unicellular spore forming protozoan microsporidians. For instance, Toguebaye et al. (2014) described *Nosema podocotyloidis* n. sp. (Microsporidia), a hyperparasite of *Podocotyloides magnatestis* (Trematoda), a parasite of *Parapristipoma octolineatum* (Teleostei) and listed 5 other species of microsporidians infecting other trematode systems. In acanthocephalans, Buron et al. (1990) demonstrated infection and pathological alterations within the acanthocephalan *Acanthocephaloides propinquus* (Dujardin, 1845) Meyer, 1933 attributable to the microsporidian hyperparasite *Microsporidium acanthocephali* Loubes, Maurand, de Buron, 1988. Stentiford et al. (2013) provided a review of microsporidian hyperparasites in helminth and other biological systems. We are not certain of the specific identity of the microsporidian infections that we observed in the body cavity of female *C. globocaudatus* that we examined from Iran but we include TEM images at various magnifications (figures 13-18).

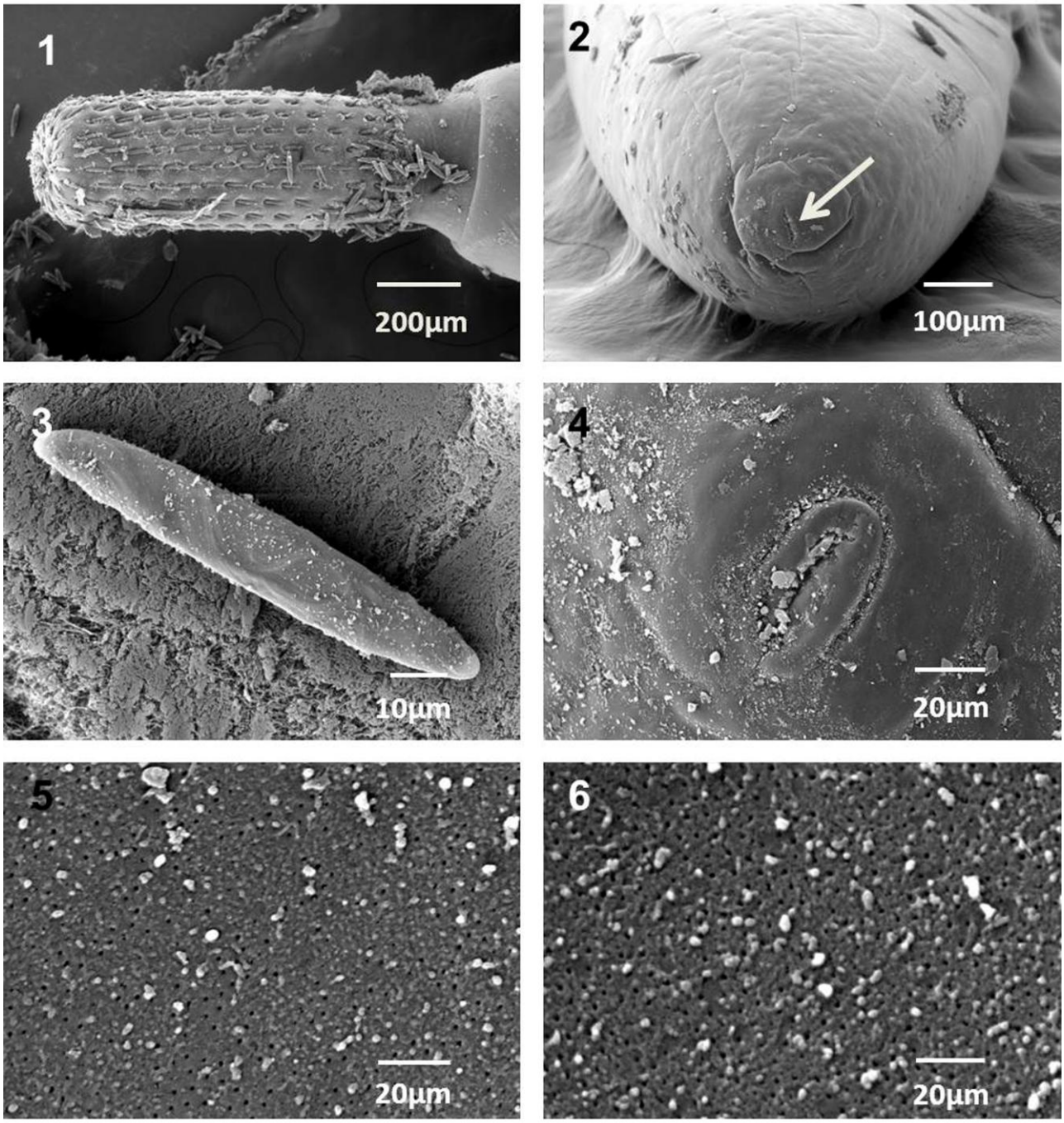

Figures 1-6. SEM of adult *Acanthocephalus rhinensis* from the intestine of *Anguilla Anguilla* in the Rhine River, Germany. 1. The proboscis of a male specimen. **2.** Posterior end of a female showing the terminal position of the gonopore. **3.** A ripe egg showing the appearance of subsurface filaments. **4.** A higher magnification of a female gonopore. **5, 6.** Micropores from the anterior and middle trunk regions, respectively. Note the difference in pore diameter and distribution.

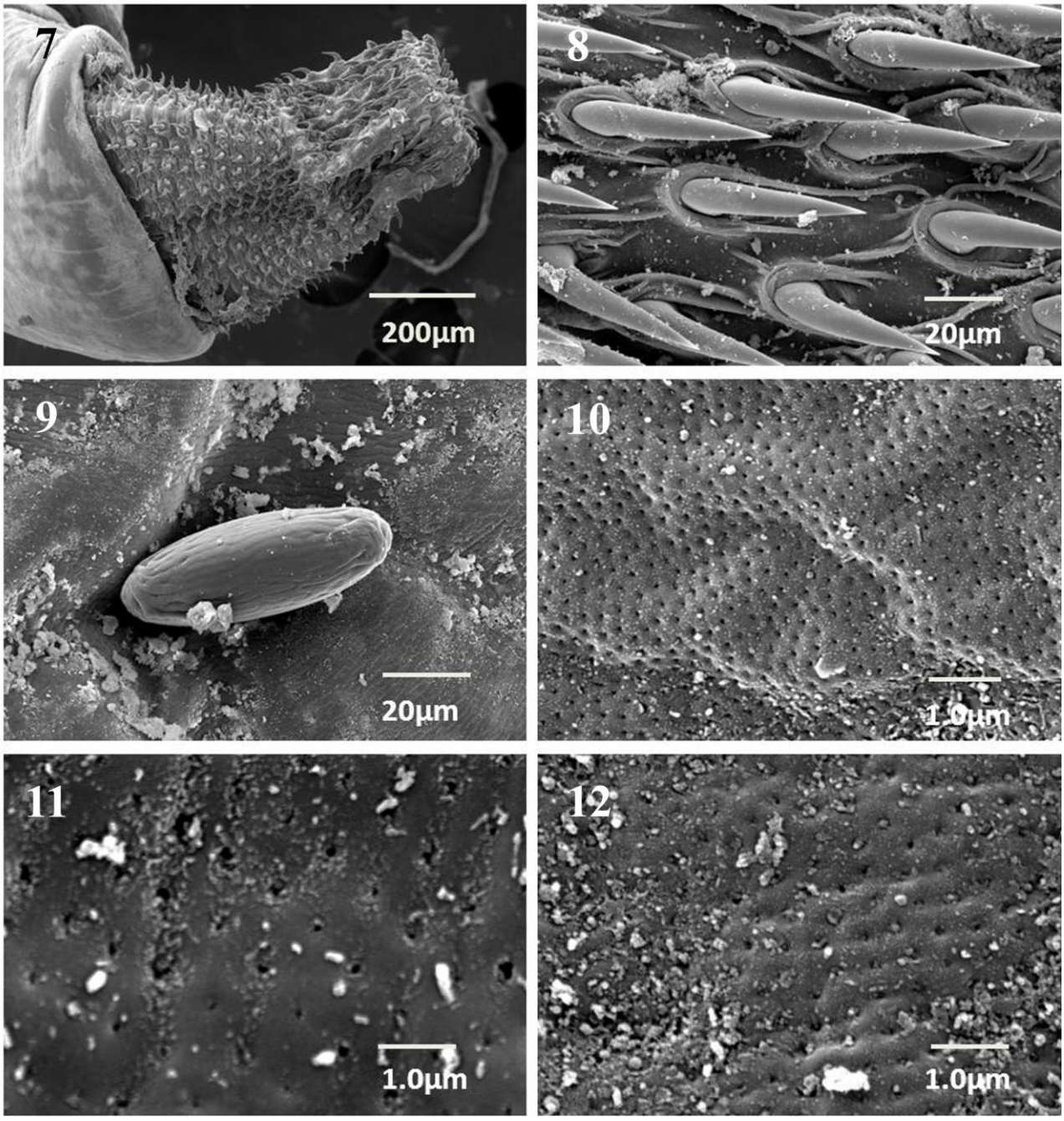

Figures 7-12. SEM of adult *Centrorhynchus globocaudatus* from the intestine of *Buteo rufinus* in Khorasan, Iran. **7.** The proboscis of a female specimen showing a partially retracted anterior part and a gradually widening posterior part. **8.** The typical form of mid-proboscis hooks embedded in elevated rims. **9.** A ripe egg featuring the inner filaments through the external surface. **10-12.** Micropores from the anterior, middle and posterior trunk, respectively, showing variations in the pore size and distribution. Anterior trunk has the most numerous and smallest pores. Middle trunk shows the fewest and largest pores with the posterior trunk being in between.

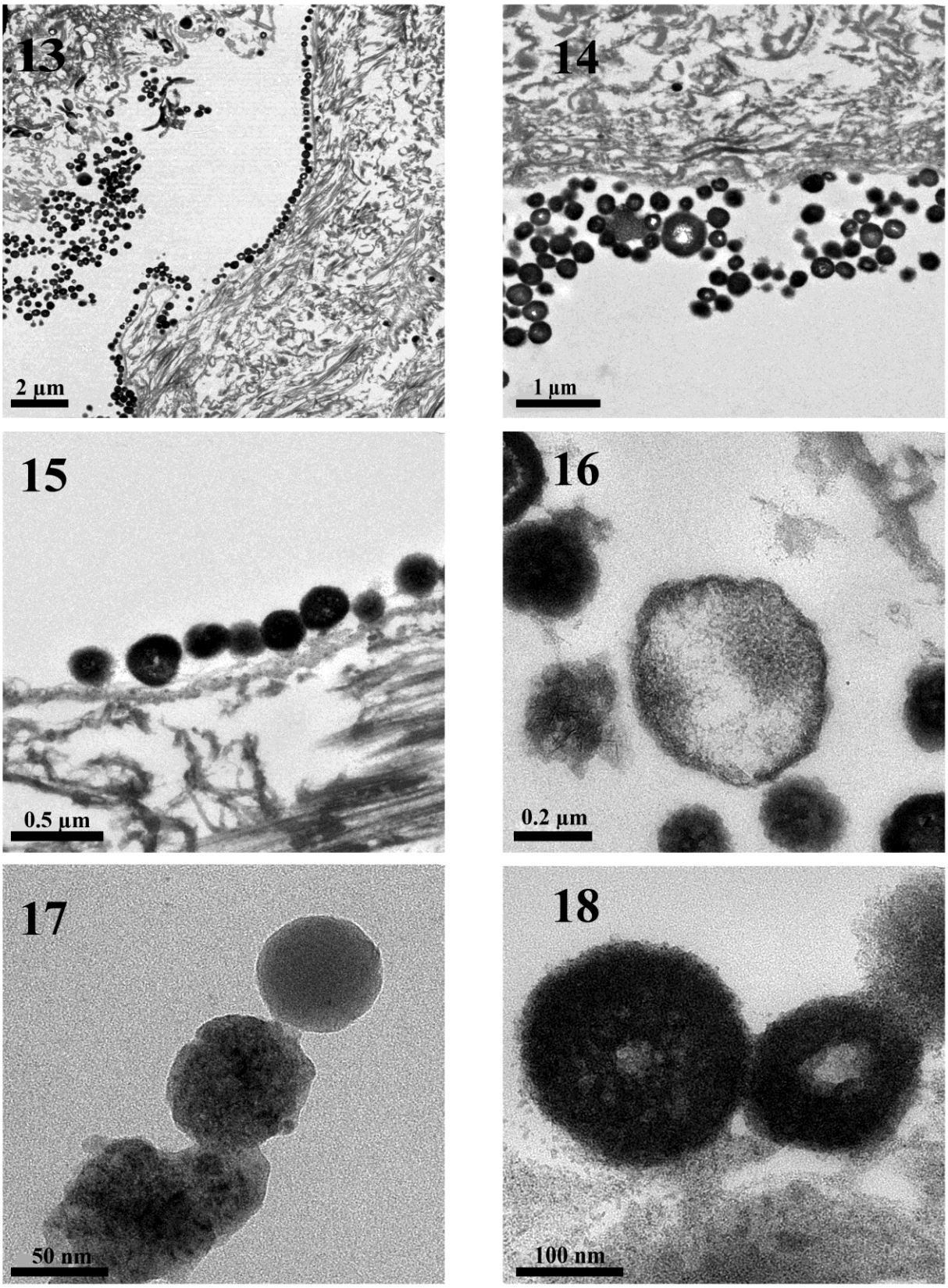

Figures 13-18. Variation in the size and organization of microsporidians from body cavity sites of female *Centrorhynchus globocaudatus* from the intestine of *Buteo rufinus* in Khorasan, Iran.

***Corynosoma strumosum* (Rudolphi, 1802) Lühe, 1904 (Polymorphidae) (figure 19)**

Amin et al. (2011) provided a comprehensive description of the morphology and histopathology of a unique population of *C. strumosum* from the Caspian seal, *Pusa caspica* (Gmelin), in the landlocked Caspian Sea using elaborate SEM and TEM images. One cross section passing through the anterior bulboid swelling was not published. That section (figure 19) details important internal structures that were not readily visualized using only light microscopy.

The most notable observations are the (1) expanded dorsal space between the cuticle and the hypoderm, (2) the presence of 2 receptacle retractors arising from the posterior end of the proboscis receptacle, (3) the organization of the transverse muscles lining the fore-trunk wall in a single band (4) lined with bands of longitudinal muscles that are considerably more prevalent dorsally than laterally or ventrally (figure 19). Aznar et al. (2018) showed that (1) the receptacle bends ventrally and is driven to the hind trunk by coordinated action of the receptacle retractors, and that (2) structural ventral bending of an inflated spiny fore-trunk with parallel rearrangement of fore-trunk muscles made attachment extremely effective in species of *Corynosoma*. Earlier, Aznar et al. (2006, p. 557) noted that "the morphological differences in trunk shape are coupled with profound disparities in muscle arrangement and attachment function" and that "the disk forming species are able to flatten their inflated fore trunk to create a spiny disk, which greatly enhances the attachment function of the proboscis." Mašová and Baruš (21013) studied the internal organization of trunk muscles of *Corynosoma pseudohamanni* Zdzitowiecki, 1984 using SEM and showed that the dorsal neck retractor muscles were not associated with the lemnisci, and that a single ventral neck retractor is present; there are 2 in our specimen (figure 19).

We have also observed microsporidian hyperinfections similar to those found in *C. globocaudatus*, in some *C. strumosum* acanthocephalans parasitizing *P. caspica* in the Caspian Sea.

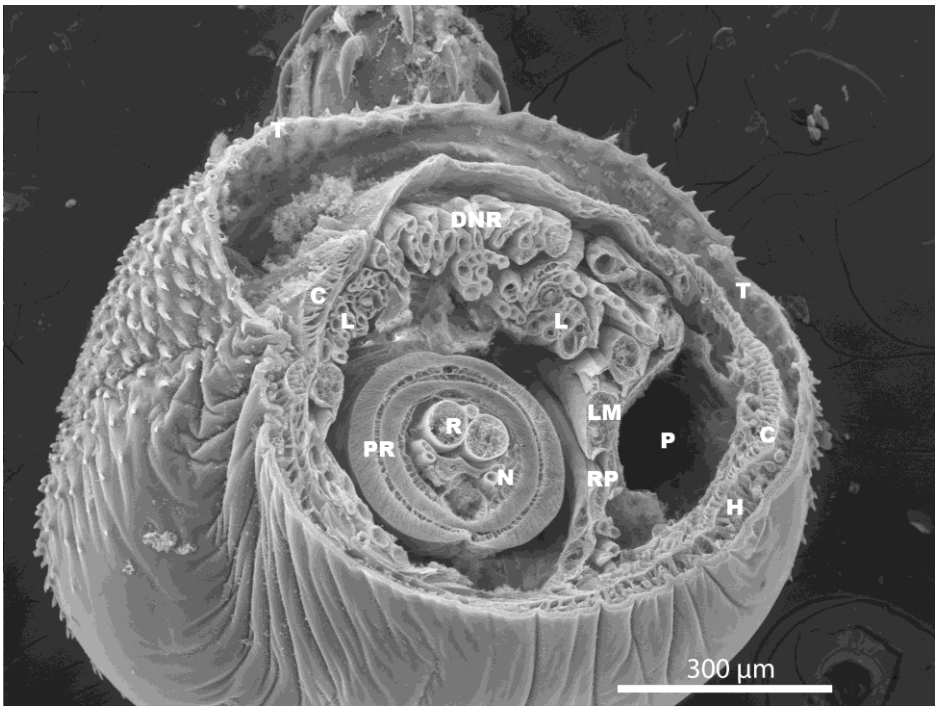

Figure 19. A razor-thin cross section of a female *Corynosoma strumosum* from *Pusa caspica* in the Caspian Sea, Iran showing major anatomical features. C: circular muscles; DNR: dorsal neck retractors; H: hypoderm; L: longitudinal muscles; LM: lemnisci; N: nerves; P: pseudocoel; PR: proboscis receptacle; R: retractor muscles of the proboscis; RP: receptacle protrusor muscles; T. Tegument.

Sphaerorostris picae **(Rudolphi, 1819) Golvan, 1956 (Centrorhynchidae) (figures 20-25)**

In 2010, we provided a comprehensive redescription of *S. picae* from magpie, *P. pica*, in northern Iran (Amin et. al., 2010). The redescription was augmented with 14 informative SEM images that did not, however, include our present figures 20-25 that add new perspectives to the better understanding of the morphology of *S. picae*.

The lateral view of the proboscis (figure 20) shows its expanding into the widening conical neck and figure 21 shows an apical perspective of the same proboscis. Figure 22 is a lateral view of hooks on the anterior proboscis showing their shape, robustness and curvature. The eggs have subdermal filaments that appear in this translucent image (figure 23). Figures 24 and 25 show new perspectives of the bursa.

Rhadinorhynchus oligospinosus **Amin, Heckmann, 2017 (Rhadinorhynchidae) (figures 26-35)**

Rhadinorhynchus oligospinosus was described from the chub mackerel *Scomber japonicus* (Scombridae) and the Chilean Jack mackerel *Trachurus murphyi* (Carangidae) from the Pacific Ocean off the Peruvian coast at the Port of Chicama, La Libertad. Amin and Heckmann (2017) found that the new species was closest to Rhadinorhynchus seriolae (Yamaguti, 1963) Golvan, 1969 found in Japanese and Australian waters, but not as close to 19 other listed species found in the same Pacific waters off Australia, Japan, and Vietnam. Eighteen SEM images were included but a few significant features were missing and are added herein to provide a full coverage of the morphology of *R. oligospinosus*. Details of the proboscis, hooks showing the serrated surface topography and the sensory pore at the neck are presented in figures 26-31.

New images of the subterminal female gonopore and orifice, eggs and a new perspective of the male bursa are added (figures 32-35).

Australorhynchus multispinosus **Amin, Heckmann, Ha, 2019 (Gorgorhynchinae) (figures 36-42)**

Three females of *Australorhynchus multispinosus* were described from the red cornetfish *Fistularia petimba* off Nha Trang, Vietnam in the Pacific south (Amin et al., 2019). It is distinguished from the only other species of the genus, *Australorhynchus tetramorphacanthus* Lebedev, 1967, by having more trunk spines extending beyond the level of the proboscis receptacle and a smaller proboscis with considerably fewer hooks. Only 5-line drawings of a whole worm, praesoma, proboscis, female reproductive system and 1 row of proboscis hooks and roots were provided by Amin et al. (2019); the measurement bar for figure 16 (p. 126) of the proboscis is herein corrected to 400 μm.

We complement this modest visual depiction with a microscope image of a proboscis (figure 36), and 6 color micrographs of an anterior hook and root (figure 37) and posterior end of female reproductive system (figure 38), and 4 images of trunk spines showing variations in the morphology of dorsal, ventral, anterior, and posterior trunk spines (figures 39-42). Anterior spines are pointed and posterior spines have rounded blunt tips and 2 support rods each.

Tenuisentis niloticus **(Meyer, 1932) Van Cleave, 1936 (Tenuisentidae) (figures 43-48)**

The description of *T. niloticus* from *H. niloticus* in Burkina Faso (Amin et al., 2016, table 1) included 12 SEM images, 6 microscope micrographs, and 5-line drawings. Aspects of internal anatomy of *T. niloticus* that were not included are added in this presentation. These included the insertion of the retractor muscles at the posterior end of the proboscis receptacle (figure 43), the cephalic ganglion (figure 44), the para-receptacle structure (figure 45), and the cement gland and related reproductive structures (figures 46-48).

The visual representation of this acanthocephalan species is now complete.

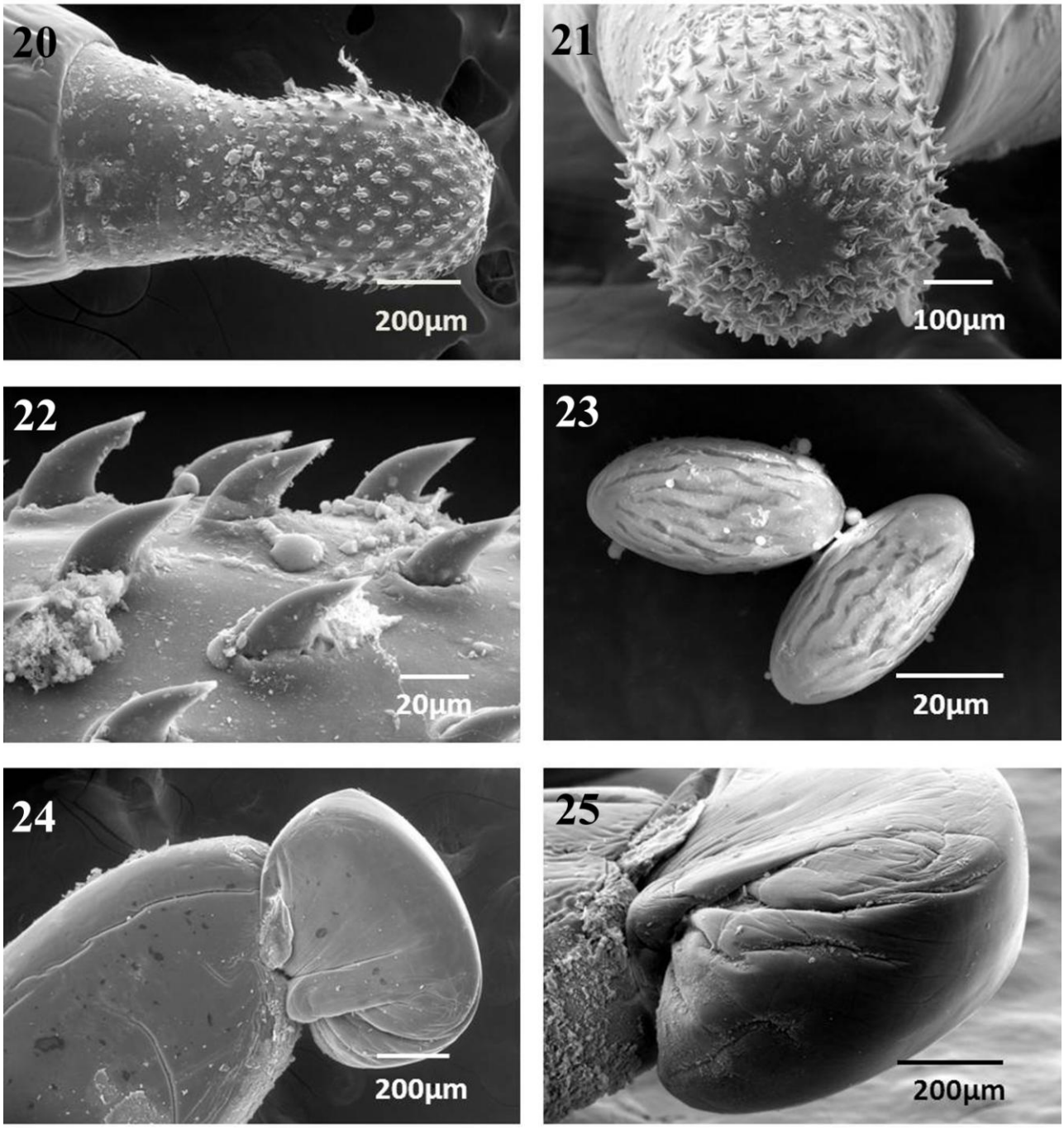

Figures 20-25. SEM of adult *Sphaerorostris picae* from the intestine of *Pica pica* in Tonekabon City, Iran. **20.** A lateral view of a female proboscis showing the ovoid shape of the anterior proboscis and a slight constriction to the widening posterior proboscis merging into the conically shaped neck. **21.** An apical view of the same proboscis in Fig. 20. **22.** A lateral view of middle hooks of the anterior proboscis showing their robustness and curvature. **23.** Two ornate eggs revealing the still intact filaments. **24, 25.** Two perspectives of the bursa.

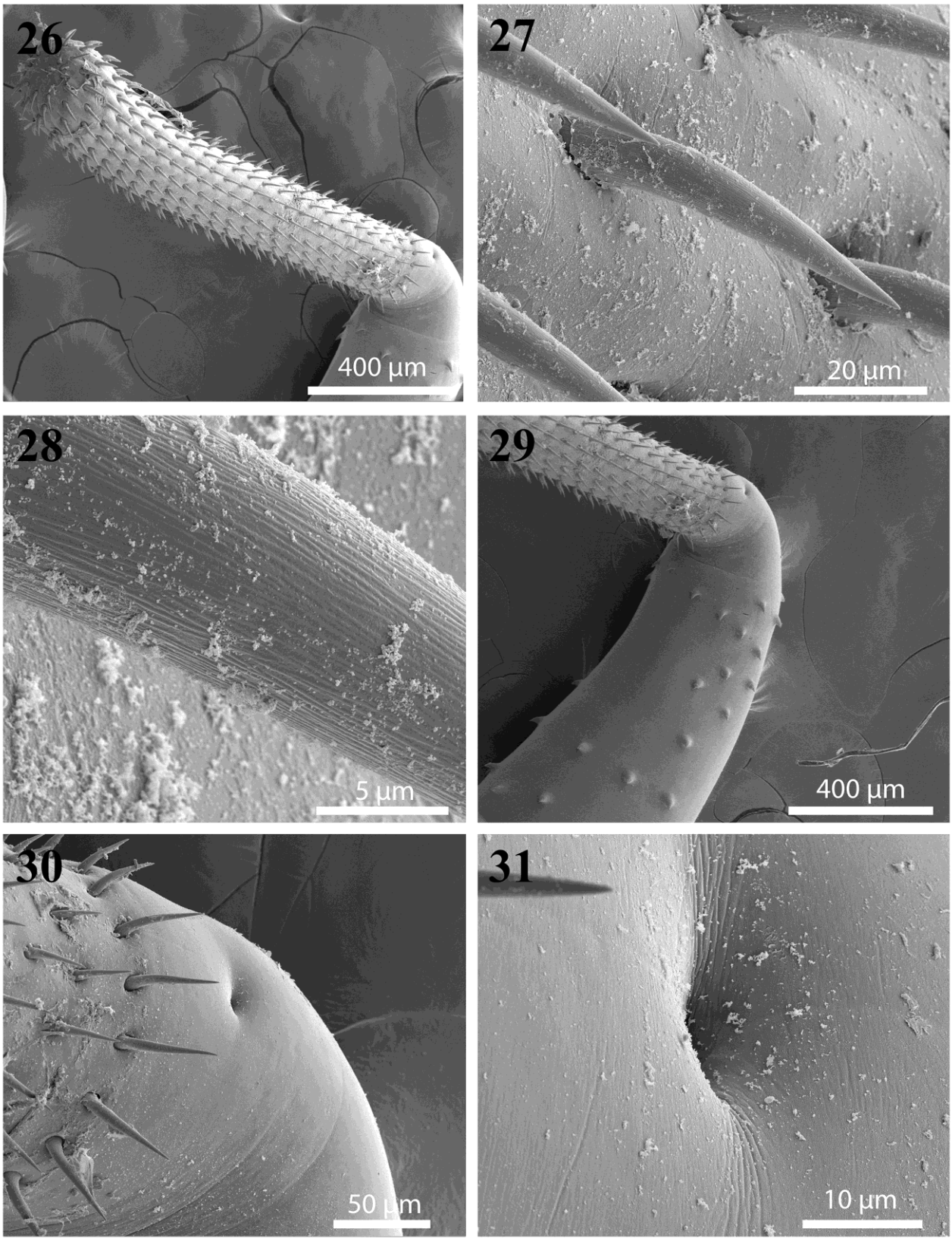

Figures 26-31. SEM of adult *Rhadinorhynchus oligospinosus* from the intestine of *Scomber japonicus* and *Trachurus murphyi* in Port Chicama, Peru. **26.** A completely everted proboscis of an adult female. **27.** Dorso-lateral hooks from the mid-proboscis. **28.** A higher magnification of a middle hook showing the characteristic serrations on the surface. **29.** The praesoma of another specimen showing the anterior trunk spines and a sensory pore on the neck. **30.** The sensory pore from specimen in Fig. 29; note the longer posterior hooks in the basal continuous ring. **Fig. 31.** A higher magnification of the sensory pore in Fig. 30.

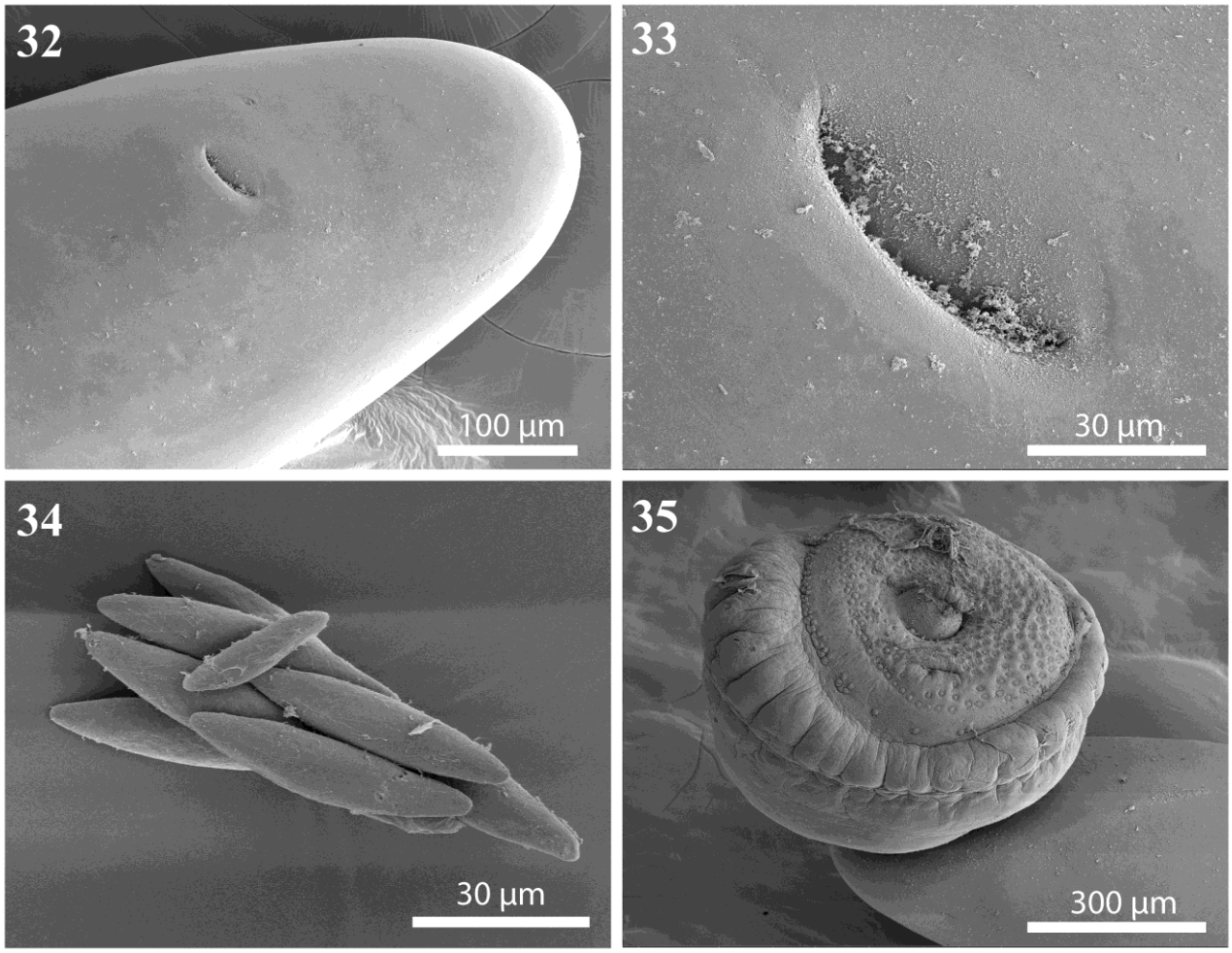

Figures 32-35. SEM of adult *Rhadinorhynchus oligospinosus* from the intestine of *Scomber japonicus* and *Trachurus murphyi* in Port Chicama, Peru. **32.** The posterior end of a female specimen showing the subventral position of the gonopore. **33.** A higher magnification of the laterally slit-like gonopore orifice from specimen Fig. 32. **34.** A few eggs at different stages of maturity. **35.** A new perspective of the male bursa showing the undulating rim, organization of the various circular pattern of sensory domes, and the penis.

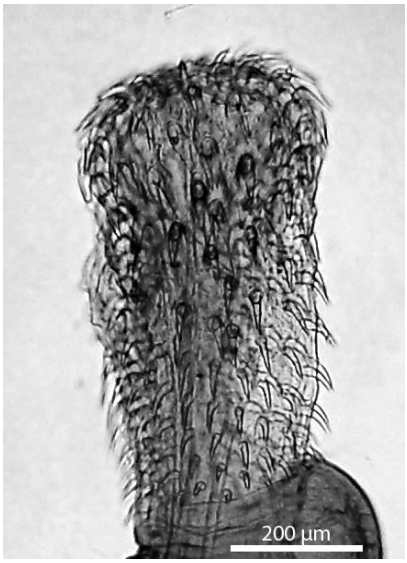

Figure 36. A new microscope image of the proboscis of an adult female *Australorhynchus multispinosus* from the intestine of *Fistularia petimba* in Vietnam; the best available microscope image.

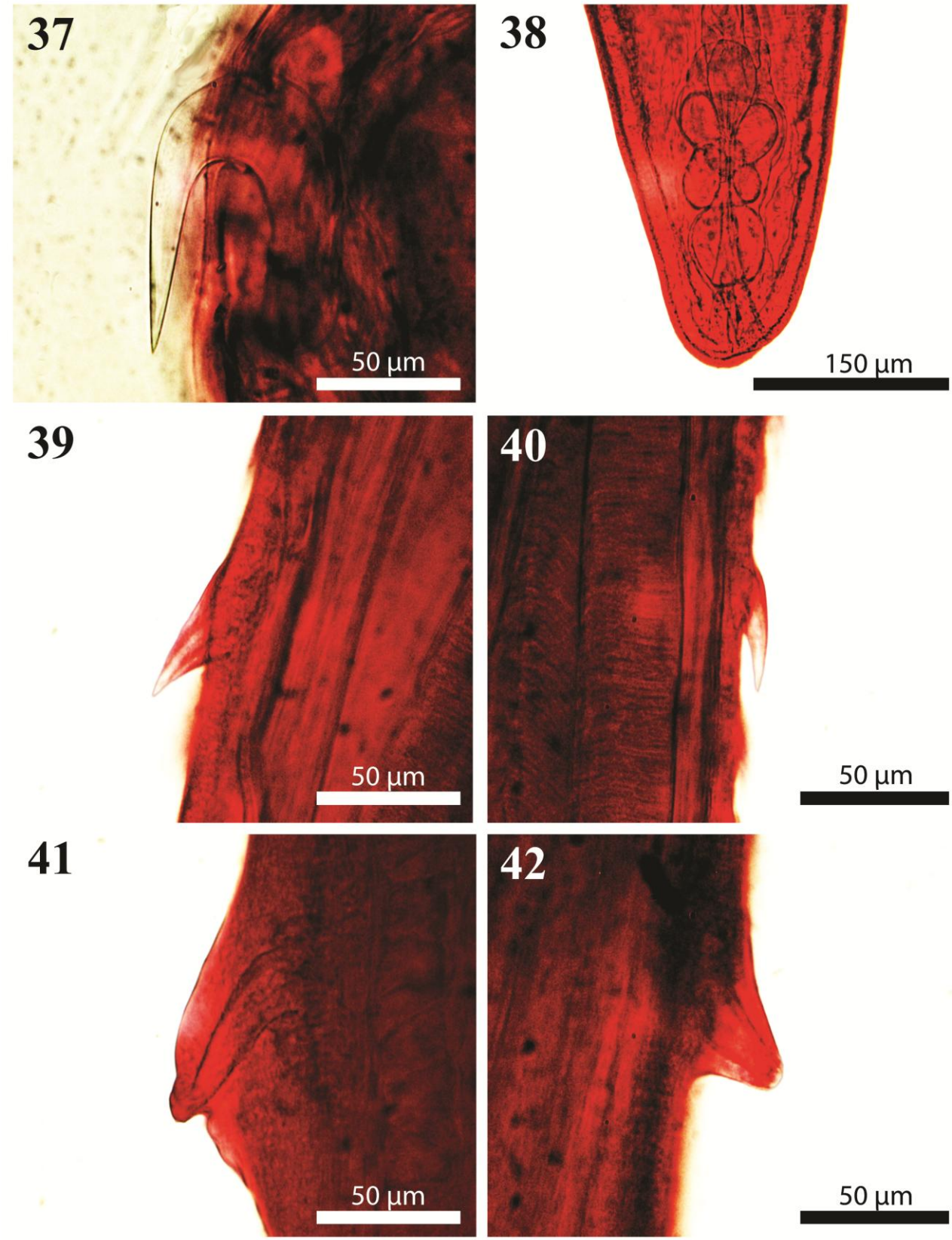

Figures 37-42. New microscope images of adult female *Australorhynchus multispinosus* from the intestine of *Fistularia petimba* in Vietnam. **37.** Lateral view of 3rd hook from anterior showing the massive posteriorly directed root. **38.** The posterior portion of a female reproductive system. **39.** Dorsal anterior trunk spine. **40.** Ventral anterior trunk spine. **41.** Dorsal posterior trunk spine. **42.** Ventral posterior trunk spine. Note the bluntness of posterior spines and their double rod support cores.

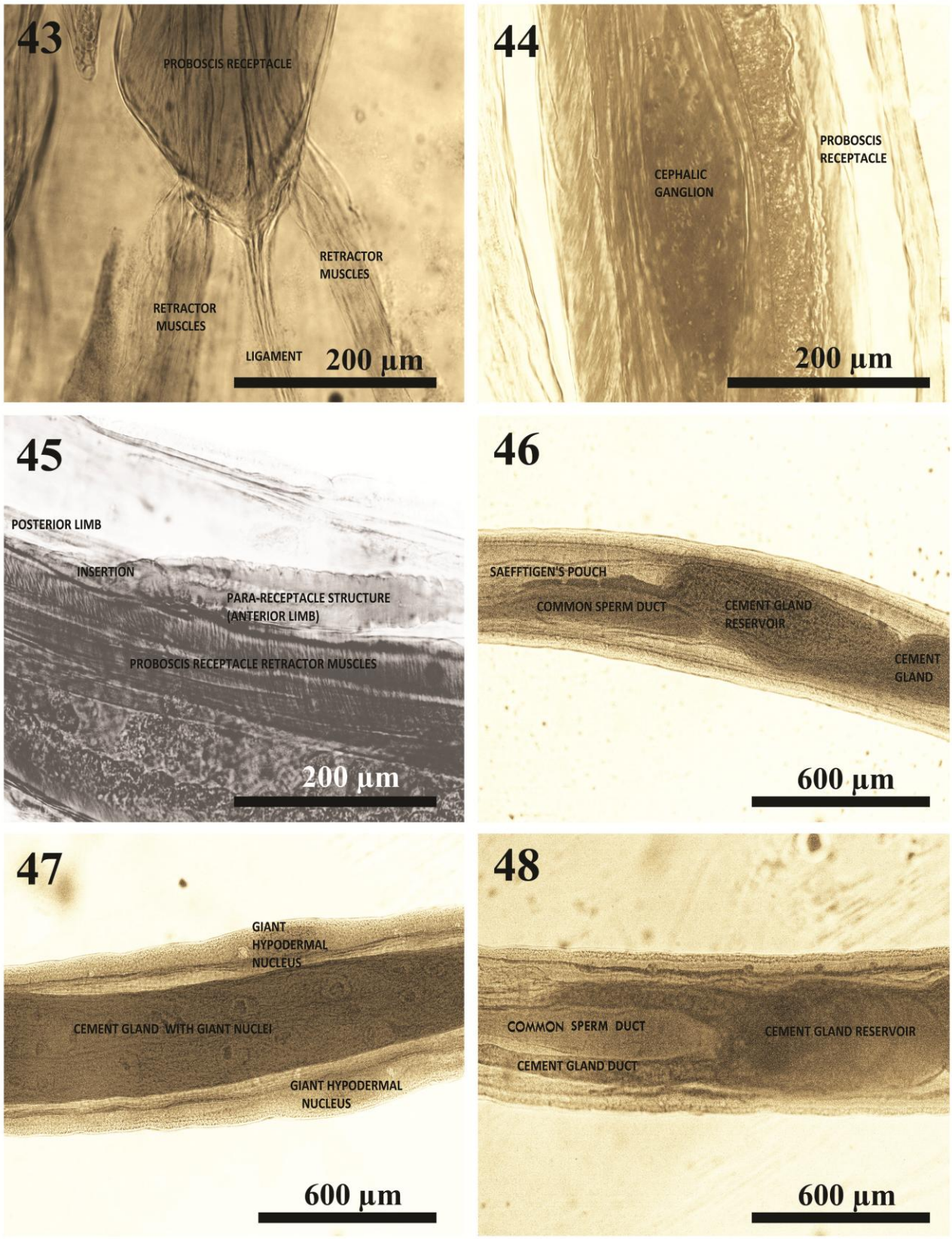

Figs. 43-48. New microscope images of adult *Tenuisentis niloticus* from the intestine of *Heterotis niloticus* in Burkina Faso. **43.** The insertion of the retractor muscles into the posterior receptacle. **44.** The cephalic ganglion. **45.** The parareceptacle structure. **46.** The relationship between the cement gland, cement gland reservoir, common sperm duct, and Saefftigen's pouch. **47.** The giant nuclei of the cement gland. **48.** The branching of the cement gland reservoir.

Concluding remarks

This report addresses visual aspects of the descriptions of 7 species of acanthocephalans that were not included in the original published work. Editors often requested smaller submissions with fewer pages to conserve space. We usually have many visuals, especially SEM images. "Biol it down" was an often-conveyed message. Our restricted submission of visuals did not do justice to the completeness of coverage of information that we have generated. This report, additionally, includes a different set of new information not previously published such as the microsporidians hyperparasites of *C. globocaudatus*, the anatomy of *C. strumosum* in a cross section, and the spines and hooks of *A. multispinosus.*

Acknowledgements

This project was supported by the Department of Biology, Brigham Young University (BYU), Provo, Utah, and by an Institutional Grant from the Parasitology Center, Inc. (PCI), Scottsdale, Arizona. Dr. Richard A. Heckmann (deceased) (BYU) and Michael Standing, Electron Optics Laboratory (BYU) created and contributed the original SEM images used. We thank Madison Laurence, Bean Museum (BYU)) for expert help in the preparation and organization of the original plates and figures. We are also grateful to Dr. Nataliya Rubtsova (PCI), and Elisabeth Trimble (BYU) for help in the preparation and organization of the presented plates and figures and to Dr. Ali Halajian, Elanco Animal Health, South Africa and formerly at the University of Limpopo, Polokowane, South Africa, for sending the specimens of *Centrorhynchus globocaudatus* from Iran.

Compliance with ethical standards

Conflict of interest. The authors declare no conflicts of interest.

Ethical approval. The authors declare that they have observed all applicable ethical standards.

References

Amin O.M., Heckmann R.A., Halajian A., Eslami A. 2010. Redescription of Sphaerirostris picae (Acanthocephala: Centrorhynchidae) from magpie, *Pica pica,* in Northern Iran, with special reference to unusual receptacle structures and notes on histopathology. J. Parasitol. 96:561-568.

Amin O.M., Heckmann R.A., Halajian A., El-Naggar A.M. 2011. The morphology of an unique population of *Corynosoma strumosum* (Acanthocephala, Polymorphidae) from the Caspian seal, *Pusa caspica*, in the land-locked Caspian Sea using SEM, with special notes on histopathology. Acta Parasitol. 56:438–445; ISSN 1230-2821

Amin O.M. Evans R.P., Boungou M., Heckmann R. 2016. Morphological and molecular description of *Tenuisentis niloticus* (Meyer, 1932) (Acanthocephala: Tenuisentidae) from *Heterotis niloticus* (Cuvier) (Actinopterygii: Arapaimidae), in Burkina Faso, with emendation of the family diagnosis and notes on new features, cryptic genetic diversity and histopathology. Syst. Parasitol. 93:173–191.

Amin O.M., Heckmann R.A. 2017. *Rhadinorhynchus oligospinosus* n. sp. (Acanthocephala, Rhadinorhynchidae) from mackerels in the Pacific Ocean off Peru and related rhadinorhynchids in the Pacific, with notes on metal analysis. Parasite 24:19.

Amin O.M. Heckmann R.A., Ha N.V. 2019. Descriptions of two new acanthocephalans (Rhadinorhynchidae) from marine fish off the Pacific coast of Vietnam. Syst. Parasitol. 96:117-129. DOI 10.1007/s11230-018-9833-x

Amin O.M., Heckmann R.A., Dallarés S., Constenla M., Rubini S. 2020. Description and molecular analysis of an Italian population of Centrorhynchus globocaudatus (Zeder, 1800) Lühe, 1911 (Acanthocephala: Centrorhynchidae) from Falco tinnunculus (Falconidae) and Buteo buteo (Accipitridae). J. Helminthol. 94:1–21. https://doi.org/10.1017/S0022149X20000887

Amin O.M., Thielen F., Münderle M., Taraschewski H., Sures B. 2008. Description of a new echinorhynchid species (Acanthocephala) from the European eel, Anguilla anguilla, in Germany, with a key to species of Acanthocephalus in Europe. J. Parasitol. 94:1299–1304. doi:10.1645/GE-1561.1

Aznar F.J., Pérez-Ponce de León G., Raga J.A. 2006. Status of *Corynosoma* (Acanthocephala: Polymorphidae) based on anatomical,

ecological, and phylogenetic evidence, with the erection of *pseudocorynosoma* n. gen. J. Parasitol. 92:548-564.

Aznar F.J., Hernández-Orts J.S., Raga J.A. 2018. Morphology, performance and attachment function in Corynosoma spp. (Acanthocephala). Parasites and Vectors 11:633. https://doi.org/10.1186/s13071-018-3165-1

Buron I. de, Loubes C., Maurand J. 1990. Infection and pathological alterations within the acanthocephalan *Acanthocephaloides propinquus* attributable to the microsporidian hyperparasite *Microsporidium acanthocephali*. Trans. Amer. Microsc. Soc.109:91–97.

Dezfuli B.S., Lui A., Squerzanti S., Lorenzoni M., Shinn A.P. 2012. Confirmation of the hosts involved in the life cycle of an acanthocephalan parasite of *Anguilla anguilla* (L.) from Lake Piediluco and its effect on the reproductive potential of its amphipod intermediate host. Parasitol. Res. 110:2137–2143. DOI 10.1007/s00436-011-2739-z

Heckmann R.A., Amin, O.M., El-Naggar A.M. 2013. Micropores of Acanthocephala, a scanning electron microscopy study. Sci. Parasitol. 14: 105-113.

Lee R.E. 1992. Scanning Electron Microscopy and X-Ray Microanalysis. 458 pp. New Jersey, Prentice Hall, Englewood Cliffs.

Mašová Š., Baruš V. 2013. Redescription of cystacanths of *Corynosoma pseudohamanni* Zdzitowiecki, 1984 (Acanthocephala: Polymorphidae) from paratenic fish hosts. Folia Parasitol. 60:169–176

Stentiford G.D., Feist S.W., Stone D.M., Bateman K.S., Dunn A.M. 2013. Microsporidia: diverse, dynamic, and emergent pathogens in aquatic systems. Trends in Parasitol. 29:567-578.

Toguebaye B.S., Quilichini Y., Diagne P.M., Marchand B. 2014. Ultrastructure and development of *Nosema podocotyloidis* n. sp. (Microsporidia), a hyperparasite of *Podocotyloides magnatestis* (Trematoda), a parasite of *Parapristipoma octolineatum* (Teleostei). Parasite 2014, 21, 44 DOI: 10.1051/parasite/2014044